

## **General Disclaimer**

### **One or more of the Following Statements may affect this Document**

- This document has been reproduced from the best copy furnished by the organizational source. It is being released in the interest of making available as much information as possible.
- This document may contain data, which exceeds the sheet parameters. It was furnished in this condition by the organizational source and is the best copy available.
- This document may contain tone-on-tone or color graphs, charts and/or pictures, which have been reproduced in black and white.
- This document is paginated as submitted by the original source.
- Portions of this document are not fully legible due to the historical nature of some of the material. However, it is the best reproduction available from the original submission.

NASA-CR-145817 ~~7~~

(NASA-CR-145817) ANALYSIS OF FOURTH  
SOUNDING ROCKET HEAT PIPE EXPERIMENT,  
SUMMARY REPORT Summary Report, Mar. - Jun.  
1974 (Brennan (Patrick), Owing Mills, Md.)  
19 p HC \$3.25

N76-13433

Unclass  
33351

CSCI 20E G3/34

SUMMARY REPORT  
FOR  
ANALYSIS OF FOURTH SOUNDING ROCKET  
HEAT PIPE EXPERIMENT

April, 1975

Prepared for

NATIONAL AERONAUTICS AND SPACE ADMINISTRATION

GODDARD SPACE FLIGHT CENTER

GREENBELT, MD. 20771

Under

Contract No. NAS5-90561/165

Prepared by

Patrick J. Brennan



## 1.0 INTRODUCTION

This report describes the work performed in support of the "Fourth Sounding Rocket Heat Pipe Experiment" during the period March, 1974 through June, 1974. The major emphasis during this period was directed toward preparing the Experiment for Integration Test. Test support and evaluation was provided during component acceptance tests, and post assembly and pre-integration tests at GSFC and at the Launch Complex at White Sands, New Mexico. A substantial part of the test effort was devoted to establishing reliable start-up and operational data for the cryogenic axial-groove methane heat pipe and its reference control pipe. Related tests were also performed with an axial-groove nitrogen heat pipe. Finally, an analysis was performed to determine the requirements and applicability of cryogenic heat pipes to NASA coolers.

## 2.0 TECHNICAL DISCUSSION

The Fourth Sounding Rocket Heat Pipe Experiment consists of two piggyback payloads carrying 14 heat pipes and experiments. Also included are three control pipes. The Experiment was launched aboard a Black Brant Sounding Rocket on October 4, 1974; more than 6-minutes of "0-g" flight time were achieved. This report describes work performed during the March, 1974 through June, 1974 period; at which time the payload was being prepared for launch in late May - early June. Problems encountered in the field with certain timer and command functions forced a launch postponement until October.

## 2.1 Experiment Description

The individual experiments and control pipes are summarized in Table 2-1. Two of the control pipes are plain aluminum tubes which have a 1.27-cm O. D. and are 91.5-cm. long. The third control pipe is a flat plate similar to the flat plate heat pipe, but without a wick. Basic heat pipe geometries include: ATS - axial groove aluminum extrusions (4); arterial pipes with and without priming foils (7); flat plate heat pipes (1); and flexible heat pipes (2). Also included as part of the GFW Experiment is an aluminum vapor chamber and a phase exchange material (PCM) aluminum heat sink. The PCM is eicosane which is used to provide temperature stability at approximately 37°C. Ammonia, acetone and methanol are used in the ambient temperature pipes, and methane is the cryogenic working fluid.

The prime objectives of the Experiment are to demonstrate "o-g" start-up and operation, and to establish "o-g" performance characteristics including start-up times, heat transport limits, and thermal conductances. A total of 172 thermistor divider networks is used to monitor the temperature data from the individual experiments. Output telemetry is 0-5VDC analog. Power is derived from a 30-VDC Ni-Cad battery. Programmed timers and command functions are used to establish the individual experiment heater power profiles. Selected heaters are also controlled by thermostats to avoid excessive temperatures. A breakdown of the instrumentation is presented in Table 2-1.

In addition to the temperature measurements, movie cameras are used to record the performance of the Photographic Pipe and Flat Plate Heat Pipe. The Photo Pipe is an axial groove geometry which has a transparent section that covers half of the circumference of the con-

TABLE 2-1. FOURTH SOUNDING ROCKET HEAT PIPE EXPERIMENT DESCRIPTION

Experimenter	Type of Pipe	No. of Pipes	EVAP up/down	Payload Section	Heater Power (Watts)	Heater Voltage Reg. (volts)	No. of Thermistors	Thermo-stats	on/off Signals	Commands
ESRO F1	Straight	1	down	B	40	28 $\pm$ 1	14	2/140°F	3	2
ESRO F2	"	1	down	B	20	28 $\pm$ 1	11	2/140°F	3	2
GSFC	flat plate/axial	2	down	B	30	28 $\pm$ 5	17	1/50°C	1	0
Hughes A	flexible	1	up	A	10		6		3	1
Hughes B	"	1	down	A	10		6		3	1
Grumman	cryogenic	1	up	A	25	28 $\pm$ 1	8	2/80°K	2	1
Grumman	pryo-control	1	up	A	25	28 $\pm$ 1	7	2/80°K	2	0
NASA/AMES A	straight	1	up	A	100	unreg	10	2/140°F	1	2
NASA/AMES B	"	1	up	A	100	unreg	10	2/140°F	1	2
NASA/GSFC	extruded groove A	1	up	B	140	unreg	8	2/140°F	3	1
NASA/GSFC	extruded groove B	1		B	100	unreg	8	2/140°F	2	1

NASA/GSFC	Flat plate	1	up	B	25/15	unreg	14	2/140°F	2	1	2	1
NASA/GSFC	Flat plate control	1	up	B	30	unreg	14	2/140°F	2	0	2	0
"	Photo	1	up	A	20/50	unreg	8	2/140°F	2	0	2	0
"	Slab A	1	up	A	100	unreg	13	2/140°F	3	1	3	1
"	Slab B	1	up	A	300	unreg	13	2/140°F	2	1	2	1
"	Ambient Control	1	up	B	75	unreg	5	2	2	0	2	0

denser section. The objective here is to observe the profiles of liquid and possibly gas slugs as they accumulate in the condenser. A number of different liquid crystal patterns were applied to the heat input side of the Flat Plate. The color response of these crystals to temperature is used to establish the transient thermal behavior of this heat pipe.

## 2.2 Test Support

During the period March, 1974 through May, 1974, the Experiment was being prepared for a late May-early June launch. Engineering support was provided during the pre-launch preparation to evaluate component and systems tests procedures and test results. The major effort was in support of the Cryogenic Experiment, and further discussions will be limited to the work related to this system.

The Cryogenic Experiment consists of an ATS-axial groove extruded aluminum heat pipe and a reference control pipe. Both pipes are charged with methane and are attached to a common aluminum heat sink. Once mounted within the payload housing (cruciform section), the entire experiment is covered with foam insulation. A multi-layer aluminized mylar insulation blanket is placed around the outside of the foam to guard against radiation from the hot payload cannister during flight. In addition to component verification tests conducted prior to installation, various tests were performed to establish telemetry calibration, transient cooldown and start-up, and normal operation.

### 2.2.1 Telemetry Calibration

Thermocouples attached adjacent to the flight thermistors were used to establish the temperature calibrations for the individual telemetry channels. Liquid nitrogen from a dewar attached to the ex-

periment heat sink was used to cool the experiment to approximately 100°K. Once temperatures stabilized near 100°K, the liquid nitrogen was turned off and the system was allowed to rise in temperature at a rate consistent with parasitic heat inputs from the ambient. Temperatures and output telemetry voltages were recorded simultaneously as the system increased in temperature to 160°K. This then established the temperature versus voltage calibrations for the telemetry networks. The calibrations were essentially linear for all channels between 100 and 130°K, increasing from approximately 1.5 to 3.5 volts over this range. The corresponding sensitivity is about 0.06 volts/°C.

#### 2.2.2 Transient Cooldown and Start Up

The Cryogenic Experiment requires that the system be cooled to approximately 100°C just before launch. Methane has a freezing point of 88.7°K and its critical temperature is 191.1°K. Consequently, if the system was cooled much below 100°K, the vapor losses associated with transporting the parasitic heat leaks were sufficiently large to cause "dry-out" at the upstream end of the evaporator. Too much cooling would ultimately result in freezing the methane in the condenser section. Large gradients between the evaporator and condenser ends would result in long start-up times which could have exceeded the 6-minute "o-g" flight time. Hence, overcooling was to be avoided. On the other hand, although less significant, if the experiment were inadequately cooled, the temperature could rise to a level above which "burn-out" would occur when subjected to flight power profiles. The 100°K start-up level proved workable, and was accomplished by On-Off regulation of the liquid nitrogen.

the 90 - 110°K range. Details of the tests and test results are presented in Ref. 2. Basically, because of the relatively low static height for nitrogen with this groove geometry ( $\leq 0.25$ -cm in the 90 - 110°K range), there was a tendency for puddling to occur even at very slight elevations. This puddling tended to obscure the performance and did not permit reliable extrapolation to "0-g" transport limits. The results point up the need for grooves which provide greater static heights (i.e. smaller effective pumping radius) if this geometry is to be used in applications below 100°K.

#### 2.4 Application of Heat Pipes to NASA Cryogenic Coolers.

An analysis was performed and available test data reviewed to determine the applicability of "state-of-the-art" cryogenic heat pipes to NASA radiant coolers, which operate in the 80 - 100°K range. The results of this study are published in Ref. 3, which is provided as Attachment A.

In general heat pipes offer a number of practical advantages in cryogenic radiant cooler systems. However, the parasitic heat loads to the heat pipes require cooler sizes larger than presently used by NASA in the 80 - 100°K temperature range. An optimum heat pipe/radiant cooler will utilize heat pipes that are as small as practical consistent with satisfying transport requirements. The "1-g" test requirements will generally dictate the heat pipe's design. Projected transport requirements for heat pipes in cryogenic NASA coolers are approximately 3 w-m. This requirement along with the need to obtain meaningful "1-g" test results leads to composite wick designs. Axial grooves might also be used but they would have to be designed to provide 2-3 times more pumping in order to avoid "1-g" puddling and obtain good test results in

### 2.2.3 Normal Operation

Tests were also conducted to establish the operation of the system with flight heat loads applied. These tests were conducted with the system in a vertical reflux mode and horizontal. The horizontal tests give close simulation of "o-g" behavior, whereas the vertical tests were performed to establish baseline data for the vertical test conducted prior to launch when the rocket and payload were in the tower. The Cryogenic Experiment is oriented in the reflux mode in the payload to avoid excessive dry out which as mentioned before would inhibit start up.

Both pipes have approximately 65-watts applied for the first 60 seconds in "o-g". This heat load along with the parasitic heat input is sufficient to evaporate all of the fluid inventory in 60 seconds, and will cause a partial dryout of the pipe. It is applied to permit a demonstration of "o-g" cryogenic start-up. After the first 60 seconds a nominal heat load of 14 watts is applied to each pipe.

A detailed discussion of the performance of this experiment is presented in Ref. 1.

### 2.3 Nitrogen Axial Groove Heat Pipe Tests

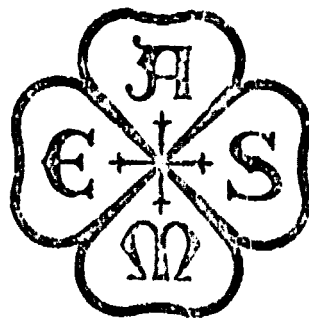
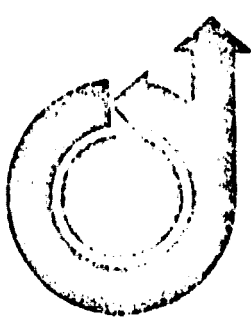
Ground tests were conducted with an ATS-axial groove extrusion charged with nitrogen to further characterize the behavior of this geometry with cryogenic fluids. The tests were conducted in a vacuum chamber at the GSFC Thermal Laboratory. The tests consisted of obtaining maximum heat transport versus elevation data for operation in

1. Harwell, W., et al. "Cryogenic Heat Pipe Experiment: Flight Performance on a Sounding Rocket," AIAA Paper No.75-729, May, 1975.

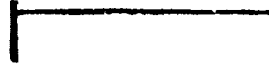
the 80 - 100°K range.

Nitrogen and oxygen are the best fluids for operation over these temperatures. An analysis was performed to determine their performance with an optimized composite slab geometry. The composite slab was selected over an arterial design because it can provide more reliable priming. Results of the analysis indicate that a 1.27-cm O.D. pipe will be required to meet the 3 w-m transport with nitrogen. Although approximately 8 w-m can be obtained with this pipe at 80°K, its performance becomes marginal at 95°K. Oxygen on the other hand can provide an optimized performance of 30 w-m at 80°K which decreases to 19 w-m at 100°K with a 1.27-cm pipe. Even with oxygen, however, the 3 w-m requirement can only be satisfied over the temperature range with pipe diameters of 1.0-cm or larger.

2. Dennis Hewitt, Master's Thesis, University of Maryland, May, 1974.
3. Sherman, A. and Brennan, P., "Cryogenic and Low Temperature Heat Pipe/Cooler Studies for Spacecraft Application." AIAA Paper No. 74-753, July, 1974.



**AIAA Paper  
No. 74-753**



**CRYOGENIC AND LOW TEMPERATURE HEAT PIPE/COOLER  
STUDIES FOR SPACECRAFT APPLICATION**

by  
**A. SHERMAN**  
NASA Goddard Space Flight Center  
Greenbelt, Maryland  
and  
**P. BRENNAN**  
Engineering Consultant  
Owing Mills, Maryland

**AIAA / ASME 1974  
Thermophysics and Heat Transfer  
Conference**

**BOSTON, MASSACHUSETTS / JULY 15-17, 1974**

First publication rights reserved by American Institute of Aeronautics and Astronautics, 1290 Avenue of the Americas, New York, N.Y. 10019, and American Society of Mechanical Engineers, 345 East 47th Street, New York, N.Y. 10017. Abstracts may be published without permission if credit is given to author and to AIAA/ASME.

**CRYOGENIC AND LOW TEMPERATURE HEAT PIPE/COOLER  
STUDIES FOR SPACECRAFT APPLICATION**

A. Sherman  
NASA Goddard Space Flight Center  
Greenbelt, Maryland

P. Brennan  
Engineering Consultant  
Owing Mills, Maryland

Abstract

Several important conclusions can be drawn from an analysis of an 80 - 100°K radiant cooler/heat pipe system for NASA spacecraft applications. Within reasonable temperature excursions, nitrogen heat pipe fluid property variations have little effect on system performance. This allows the system to operate over a range of cooling loads with the cooler temperature controlled by a heater. The system size and weight are strongly dependent upon heat pipe length and diameter because of the parasitic load effect. Present day NASA coolers could not accommodate a practical heat pipe because of this effect, and larger heat pipe cooler systems would be required in the 80 - 100°K range. An optimized heat pipe for this system is one whose diameter is as small as practical, but consistent with the transport and priming requirements imposed by ground testing and the zero-g application. The composite slab wick configuration appears to offer a reliable, "state-of-the-art" heat pipe with adequate capacity to meet both present day and projected NASA radiant cooler applications. Heat pipe diameters on the order of 1.0 cm have theoretical transport capabilities greater than 2.5 w-m in the 80 - 100°K temperature range with conventional composite slab wicks and nitrogen or oxygen working fluids. An analysis of a solid cryogen/heat pipe/radiant cooler system indicates that, for special applications, this system provides a weight savings when compared to a two stage solid cryogenic cooler.

Nomenclature

$A_c$  Effective heat transfer area of secondary cryogen shroud

$A_p$  Radiant cooler patch area

$A_p^*$  Radiant cooler patch size for reference-point cooler

$A_{HT}$  Heat pipe parasitic load heat transfer area  
 $= \pi \lambda_{HP} l_{HP}$

$A_v$  Vapor flow area

$A_w$  Wick cross-sectional area

$D_{H,v}$  Hydraulic diameter of vapor flow

$D_{HP}$  Heat pipe diameter

$\epsilon_p$  Radiator patch emissivity

$\bar{\epsilon}$  Effective emissivity of multi-layer insulation of solid cryogen

$\bar{\epsilon}_{HI}$  Effective emissivity of multi-layer insulation around a heat pipe

$g_0$  Gravitational constant

$h$  Heat pipe elevation

$H_s$  Static elevation head

$h_s$  Heat of sublimation of primary solid cryogen

$h_s^*$  Heat of sublimation of secondary solid cryogen

$k$  Heat pipe permeability

$K_1$  Radiation heat transfer coefficient from the first stage of the cooler to the patch

$K_2$  Conduction heat transfer coefficient from the first stage to the patch for a radiant cooler

$K_3$  Thermal conductance of cooler patch mount

$K_1^*$   $K_1$  for a reference-point cooler

$K_2^*$   $K_2$  for a reference-point cooler

$K(T_p)$  Heat pipe effective conductance

$K'(T_p)$   $d[K(T_p)]/dT_p$

$l$  Length of cylindrical primary cryogen

$l_c$  Heat pipe condenser length

$l_e$  Heat pipe evaporator length

$l_{HP}$  Heat pipe length

$l_T$  Heat pipe transport length

$M^*$  Mass of secondary solid cryogen

$N_L$  Liquid transport factor

$\nu_L$  Heat pipe liquid kinematic viscosity

$\nu_v$  Heat pipe vapor kinematic viscosity

$\dot{Q}_A$  Albedo heat input

$\dot{Q}_{COND}$  Conduction load from first stage of radiant cooler to the patch

$\dot{Q}_E$  Earth heat input

ORIGINAL PAGE IS  
OF POOR QUALITY

- $\dot{Q}_{HP}$  Heat pipe parasitic load
- $\dot{Q}_L$  Cooling load (e. g. detector heat dissipation)
- $\dot{Q}_{OP}$  Optical port load
- $\dot{Q}_{RAD}$  Radiation load from first stage of radiant cooler to the patch
- $(\dot{Q}_L)_{eff}$  Heat pipe transport capability
- $(\dot{Q}_L)_{REQD}$  Heat pipe transport requirement
- $\dot{Q}_S$  Solar heat input
- $r_p$  Effective pumping radius
- $r$  Radius of cylindrical primary cryogen
- $\rho_L$  Liquid density
- $\rho_s$  Primary cryogen density
- $\sigma$  Boltzmann's Constant
- $\sigma_L$  Liquid surface tension
- $T_E$  Ambient temperature (294°K)
- $T_{HP}$  Average temperature of heat pipe
- $T_L$  Cooling load (e. g. detector) temperature
- $T_M$  Mission time
- $T_I$  Temperature of solid cryogen cooler inner shell temperature
- $T_p$  Radiant cooler patch temperature
- $T_{H1}$  Radiant cooler first stage temperature
- $T_s$  Primary solid cryogen temperature

Introduction

Potential applications for cryogenic or low temperature heat pipes aboard spacecraft include

- 1) the coupling of one or several detectors to individual or multiple passive and/or active coolers,<sup>(1)</sup>
- 2) isothermalization of radiant coolers,<sup>(1)</sup>
- 3) cryo-diode applications (e. g. Figure 1a),
- 4) coupling of optical packages to coolers, and
- 5) hybrid cooler systems (e. g. Figure 1b).

Cryogenic heat pipes might also find applications as interface components between radiators and large multiple detector arrays, or to provide for detachable detectors and/or radiators for shuttle resupply.



Figure 1a. Cryo-Diode Application

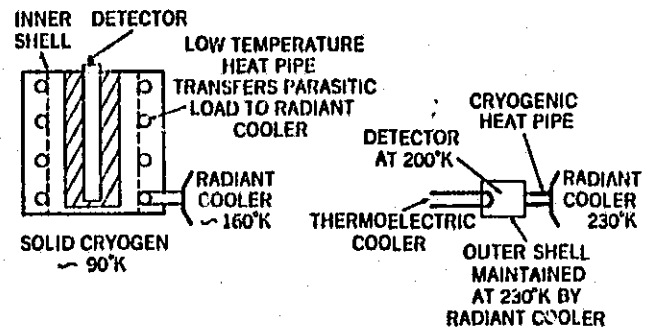


Figure 1b. Hybrid Coolers Employing Heat Pipes

A review of the literature shows an increasing amount of work on low temperature heat pipes. Brennan (2) et al. obtained 77°K data for nitrogen heat pipes with axial grooved and arterial wick configurations, while Wright (1) et al. report on the development of a low temperature heat pipe/radiator and heat pipe transport system for detector cooling. The axial groove wick geometry is employed in the latter reference, while Freon-14 is used in the radiator pipes (130°K), and methane is employed in the transporters (130 - 150°K). Murray (3) shows test data for 2-watt methane heat pipes at 110°K which employ a wire cloth wick. Extensive performance data for an extruded axial groove geometry charged with oxygen, methane and ethane and operated in the 100 - 200°K range is presented in Reference 4.

The prime purpose of the present work is to examine cryogenic heat pipe/cooler feasibility in the 80 - 100°K temperature range and in the regimes of operation required for NASA spacecraft. Present requirements within these regimes are

- 1) cooling load of less than 1-2 watts per cooler,
- 2) small detector/heat pipe interface area,
- 3) high systems reliability and long lifetime operations.

The cooling capacity of practical radiant coolers is very low in this temperature range, and very temperature sensitive. Detector performance is also strongly dependent on temperatures in this regime. It is, therefore, important to understand the interplay of the heat pipe and its effects on overall system performance. As will be developed, the heat pipes' size and thermal conductance directly impact the cooler design. Finally, a change in heat load could alter the radiant cooler temperature and thereby change the heat pipes' operating characteristics. Since candidate cryogenic fluids for the range of interest experience changes in their properties for relatively small temperature changes, it is imperative that these heat pipe characteristics be known and predictable.

As the systems part of this study developed it became clear that an evaluation of past and potential cryogenic heat pipe types was required. This was done by analysis, data review, and some new testing. Emphasis on this evaluation was put on nitrogen heat pipes, although oxygen pipes were considered. Hopefully, the results of this evaluation, together with the systems studies, will point the way towards the types of heat pipes which are practical for these low temperature range applications.

Finally, in an effort to identify possible new low temperature heat pipe/cooler systems, a brief analysis is presented to indicate the feasibility of a hybrid solid cryogen/passive cooler system which employs a low temperature heat pipe.

### Radiant Cooler/Heat Pipe System

#### General Configuration

Figure 2 shows a general schematic of a low temperature or cryogenic heat pipe/radiant cooler system.

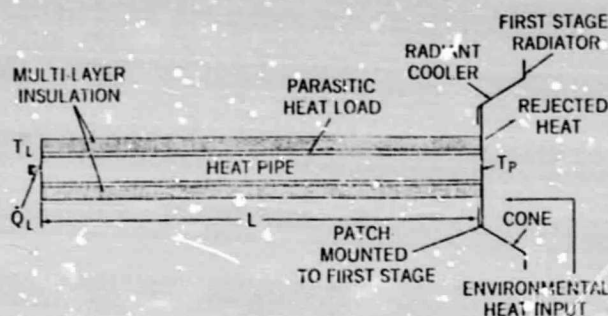


Figure 2. Schematic of Radiant Cooler/Heat Pipe System

Typically the cooler is constructed in two stages. The first stage consists of a cone with a highly reflective inner surface and a radiator which cools the cone to 170°K. The purpose of the cone is to shield the patch from the spacecraft and earth, or to reflect shallow-angle sun input out of the cooler before it reaches the patch. Further isolation from the spacecraft is obtained by mounting the patch to the first stage with low conductive supports. If shielding from the spacecraft is not required, and there is no sun input to the cooler, the second stage cone can be eliminated and a deployable door attached to the mouth of the first stage can be used to block the patch view of the earth.

For coolers presently in operation the components requiring cooling (e.g. detector) are mounted directly to the patch. The addition of a cryogenic heat pipe into the system, while allowing greater flexibility in spacecraft and instrument design, introduces new problems and limitations which must be considered.

#### Parasitic Loads

A curve of the parasitic load impressed upon a cryogenic heat pipe aboard an ambient temperature spacecraft is shown in Figure 3. The approximate heat rejection capacity of the patch of present-day NASA radiant coolers is also shown in this figure. It is clear that even for good values of multi-layer effective emissivity

(~.01), a small diameter heat pipe (e.g. 3 mm) would require a larger cooler than is presently being employed.

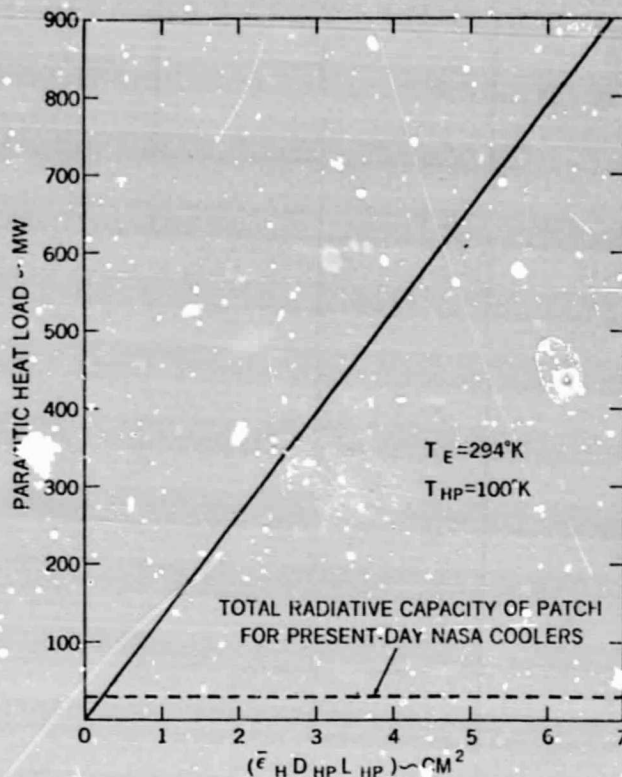


Figure 3. Parasitic Load vs.  $\bar{\epsilon}_H D_{HP} L_{HP}$

The effect of heat pipe size and parasitic load on required patch area is estimated in the following analysis for a cooler without a cone. An energy balance for the patch, neglecting earth, albedo, and solar input yields

$$\sigma \epsilon_p T_p^4 = \dot{Q}_{OP} + \dot{Q}_{COND} + \dot{Q}_{RAD} + \dot{Q}_{HP} + \dot{Q}_L \quad (1)$$

where

$$\dot{Q}_{HP} \approx \sigma \pi (\bar{\epsilon}_H D_{HP} L_{HP}) (T_E^4 - T_p^4) \quad (2)$$

and

$$\dot{Q}_{RAD} = K_1 (T_{r1}^4 - T_p^4) \quad (3)$$

$$\dot{Q}_{COND} = K_2 (T_{r1} - T_p) \quad (4)$$

Now, taking present day NASA coolers as a reference point we assume that

$$K_1 \approx K_1^* (A_p/A_p^*) \quad (5)$$

$$K_2 \approx K_2^* (A_p/A_p^*) \quad (6)$$

Combining equations (1) through (6)

$$A_p = \frac{\dot{Q}_L + \dot{Q}_{OP} + \sigma \pi (\bar{\epsilon}_H D_{HP} L_{HP}) (T_E^4 - T_p^4)}{-K_1^*/A_p^* (T_{r1} - T_p) - K_2^*/A_p^* (T_{r1} - T_p) + \sigma \epsilon_p T_p^4} \quad (7)$$

A plot of equation (7) is shown in Figure 4. The reference-point constants were taken at their values for a typical present day NASA cooler. Also, the figure shows two cases (dotted lines) which represent the extreme values for  $\bar{\epsilon}_H D_{HP} L_{HP}$  which are of interest here.

Figure 4 can be used to estimate the radiant cooler patch area required for a heat pipe/cooler system with a given optical and detector load. For example, for a present day cooler with a fixed load of about 20 mw the curves show that a 50 cm<sup>2</sup> patch is required. If a 1 meter long, 6.3 mm O. D. heat pipe with  $\bar{\epsilon}_H = .01$  is included in the system the patch area increases to 240 cm<sup>2</sup>.

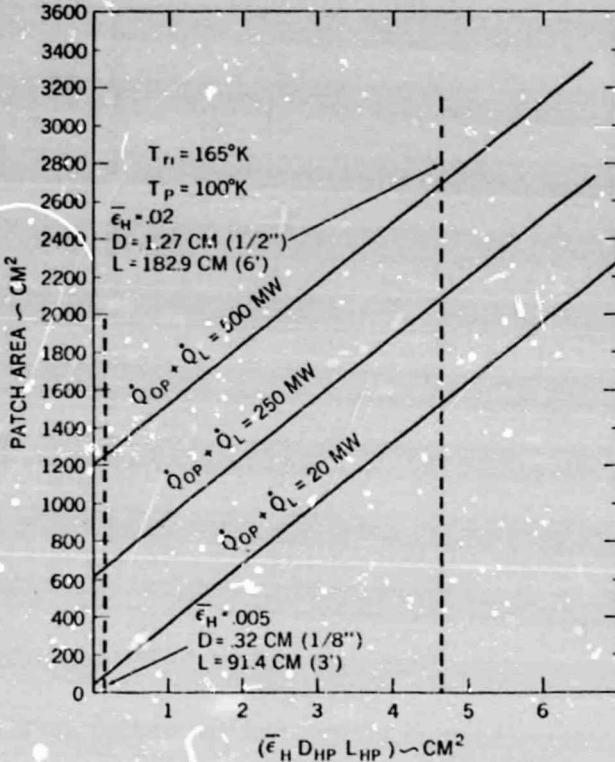


Figure 4. Radiant Cooler Patch Area vs.  $\bar{\epsilon}_H D_{HP} L_{HP}$

Figures 3 and 4 illustrate that because of the inherent parasitic loads, a cryogenic heat pipe/radiative cooler combination must be considered as a system, rather than as an addition of a cryogenic heat pipe to an existing radiator. Also, larger radiant coolers than are presently being developed are required to accommodate both the heat pipe and the larger cooling loads of future applications. Finally, it should be noted that as the cooler temperature level increases, the effect of the heat pipe on system performance becomes less significant because its parasitic losses decrease whereas the cooler capacity increases.

#### Cooler Sensitivity

The thermal conductivities of cryogenic fluids generally decrease with temperature. Therefore, a higher-than-expected cooling load would result in an increase in load temperature due to both a higher heat pipe temperature drop and an increase in radiant cooler temperature. It was felt that this interaction warranted some analysis.

An energy balance for a cooler patch (without a cone) yields:

$$\dot{Q}_{OP} + \dot{Q}_L + \bar{\epsilon}_H \sigma A_{HT} (T_E^4 - T_P^4) + K_1 (T_{H1}^4 - T_P^4) + K_2 (T_{H1} - T_P) + \dot{Q}_{ALB} + \dot{Q}_E + \dot{Q}_S = \sigma \epsilon_p A_p T_P^4 \quad (8)$$

Assuming  $T_{H1}$ ,  $\dot{Q}_{ALB}$ ,  $\dot{Q}_E$ ,  $\dot{Q}_{OP}$ ,  $\dot{Q}_S$  to be constant, taking the differential, and rearranging

$$dT_P = \frac{d\dot{Q}_L}{4\sigma \bar{\epsilon}_H A_{HT} T_P^3 + 4K_1 T_P^3 + K_2 + 4\sigma \epsilon_p A_p T_P^3} \quad (9)$$

Now, for the heat pipe in the cooler/heat pipe system

$$\dot{Q}_L + \frac{1}{2} \bar{\epsilon}_H \sigma A_{HT} (T_E^4 - T_P^4) = K(T_P) (T_L - T_P) \quad (10)$$

or

$$T_P + \frac{\dot{Q}_L}{K(T_P)} + \frac{\frac{1}{2} \bar{\epsilon}_H \sigma A_{HT} (T_E^4 - T_P^4)}{K(T_P)} = T_L \quad (11)$$

Differentiating (11) yields:

$$dT_L = \left[ \frac{d\dot{Q}_L}{K(T_P)} \right] + \left[ 1 - \frac{(\dot{Q}_L + \frac{1}{2} \bar{\epsilon}_H \sigma A_{HT} T_L^4 - \frac{1}{2} \bar{\epsilon}_H \sigma A_{HT} T_P^4) (K'(T_P))}{[K(T_P)]^2} - \frac{2\bar{\epsilon}_H \sigma A_{HT} T_P^3}{K(T_P)} \right] dT_P \quad (12)$$

Combining (9) and (12) results in

$$dT_L = \left[ \frac{d\dot{Q}_L}{K(T_P)} \right] + \left[ 1 - \frac{(\dot{Q}_L + \frac{1}{2} \bar{\epsilon}_H \sigma A_{HT} T_L^4 - \frac{1}{2} \bar{\epsilon}_H \sigma A_{HT} T_P^4) (K'(T_P))}{[K(T_P)]^2} - \frac{2\bar{\epsilon}_H \sigma A_{HT} T_P^3}{K(T_P)} \right] \left[ \frac{1}{4\bar{\epsilon}_H \sigma A_{HT} T_P^3 + 4K_1 T_P^3 + K_2 + 4\sigma \epsilon_p A_p T_P^3} \right] d\dot{Q}_L \quad (13)$$

Equation (13) shows the influence of various factors on the cooling load change in temperature. The first term in brackets is the increase in  $T_L$  due to a higher heat transfer in the heat pipe. The first term in the second set of brackets represents the increase in  $T_L$  due to an increase in  $T_P$ , while the  $K'(T_P)$  term takes into account the property change of the heat pipe fluid. The last term in the second set of brackets corrects for the decrease in parasitic load to the heat pipe with a rise in  $T_P$ .

As an example, consider the following conditions

- $\epsilon_p = .95$
- $T_{H1} = 165^\circ K$
- $T_P = 100^\circ K \sim T_{HP}$
- $\dot{Q}_{OPT} = 50 \text{ mw}$
- $\dot{Q}_L = 10 \text{ mw}$

Earth, albedo, solar input = 0

\*Assume  $T_{HP} \sim T_P$

ORIGINAL PAGE IS  
OF POOR QUALITY

$$D_{HP} = 1.27 \text{ cm}$$

$$L_{HP} = 91 \text{ cm}$$

$$\bar{\epsilon}_H = .015$$

$$A_p = 630 \text{ cm}^2 \text{ from Figure 4}$$

Working fluid - nitrogen

Then, from equation (13)

$$\frac{dT_L}{dQ_L} = .07 \text{ }^\circ\text{K/mw} \quad (14)$$

In this particular example  $dT_L/dQ_L$  is primarily dependent on patch temperature rise because the parasitic load and fluid thermal conductivity effects are small and tend to cancel out. In general, then, for nitrogen heat pipes, the load temperature is primarily a function of patch temperature and the system can readily be controlled by a heater on the patch.

From a systems viewpoint, equation (13), as well as the integrated heat balance equations (8) and (11), are useful in predicting first approximations to heat pipe/cooler performance and thermal design trade-off considerations.

#### Heat Pipe Requirements

It is obvious from the previous system's analysis that a heat pipe/radiator cooler will be optimized by using as small a diameter heat pipe as possible. In these applications, heat pipe diameters should be minimized within practical fabrication limits and the following design criteria:

- 1) Satisfy thermal conductance ( $\Delta T$ ) requirements
- 2) Satisfy "0-g" transport requirements
- 3) Permit meaningful "1-g" testing

The heat loads and consequently the temperature drops experienced in these applications are minimal. For those instances where the heat flux may be too high the diameter of the heat pipe can be enlarged in the evaporator and/or condenser section to accommodate the  $\Delta T$  requirement.

The last two criteria relate to the transport capability of the heat pipe. In this regard, because of the rather small heat loads, such limits as sonic vapor, constraint, etc., do not apply and the transport capability of the heat pipe is determined by the conventional capillary pumping limit. (6)

In order to establish whether a particular heat pipe's transport capability is adequate, one must first determine the transport requirements associated with the application. For the simple case of a single evaporator and condenser at opposite ends of the pipe with a parasitic load applied over the length of the pipe

$$(QL)_{REQD} = (\dot{Q}_{OPT} + \dot{Q}_{HP}) (\frac{1}{2}L_c) + [Q_{OPT}L_T + Q_{HP} (\frac{1}{2}L_T)] + (Q_{OPT} + Q_{HP}) (\frac{1}{2}L_c) \quad (15)$$

$$\text{where } \dot{Q}_{OPT} = \dot{Q}_{OP} + \dot{Q}_L$$

In many of these applications the evaporator and condenser lengths will be small compared to the total length and therefore a conservative approximation of the transport requirement is

$$(QL)_{REQD} \cong [Q_{OPT} + \frac{1}{2}Q_{HP}] L_{HP} \quad (16)$$

It is interesting to note that in this case, because of the significance of the parasitic heat load, the transport requirement becomes a function of  $L_{HP}^2$ , versus the linear dependence commonly experienced when parasitic losses are negligible.

The transport requirement is presented in Figure 5 versus heat pipe length with  $Q_{OPT}$  and  $(\bar{\epsilon}D)_{HP}$  as parameters. If a 2-M long  $\times$  1.27-cm O. D. heat pipe were employed in present NASA applications ( $Q_{OPT} \cong 25 \text{ mw}$ ) it would have to accommodate a transport requirement of approximately 0.55 w-m. The transport requirement for the same pipe with a projected detector load of 0.5 w would increase to 1.5 w-m.

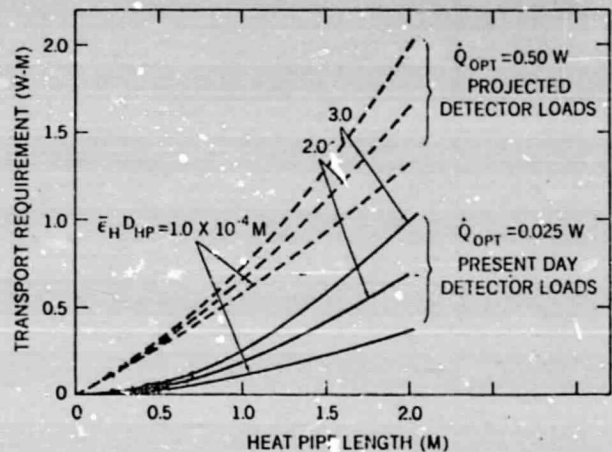


Figure 5. Transport Requirements for a Heat Pipe/Radiant Cooler System

These transport requirements are relatively low even for cryogenic fluids. The 1.27-cm O. D. axial groove and arterial heat pipes tested in Reference (2) both have measured transport capabilities with nitrogen at 80°K in excess of 15 w-m. The capacity with oxygen could be almost twice as high. Although these pipes have high transport capability, they do have inherent problems. Present day arterial pipes still have not demonstrated reliable start-up. The existing axial groove geometry has very low static heights with oxygen and nitrogen, and puddling effects obscure the "1-g" test data. (5) Homogeneous and composite slab wicks (7) have proven reliability and are potential alternatives to the artery and axial groove provided that they have adequate transport capability.

As regards the choice of working fluids, in addition to nitrogen and oxygen other candidates for the 80 - 100°K range are fluorine, carbon monoxide, argon and methane. However, fluorine and carbon monoxide present serious safety problems, argon has too narrow an operating temperature range and methane's freezing point is 88. 7°K.

Methane also experiences high vapor losses and start-up problems up to approximately 100°K. As a result, nitrogen and oxygen represent the best choice and are the only fluids considered in the subsequent analysis.

Cross sections of horizontal, homogeneous and composite slab wick designs are presented in Figure 6. The analysis neglects fillet flow and assumes that the secondary wick does not affect the transport capability of the system. With these assumptions, the transport capability ( $QL_{eff}$ ) for a slab heat pipe with uniform flow areas and wick properties is given by (6)

$$(QL_{eff}) = \frac{2kA_w}{r_p} F_\ell N_\ell (1+h) \quad (17)$$

where "perfect wetting" has been assumed and

$$F_\ell = \frac{l}{l + \frac{\nu_v}{\nu_\ell} \frac{32k}{L} \frac{A_w}{A_v}} \quad (18)$$

and for a horizontal slab geometry

$$h = - \left( \frac{r_p D_{HP}}{4\gamma} + \frac{r_p h}{2\gamma} \right) \quad (19)$$

with

$$\gamma = \frac{\sigma_\ell}{\rho_\ell g u} \quad (20)$$

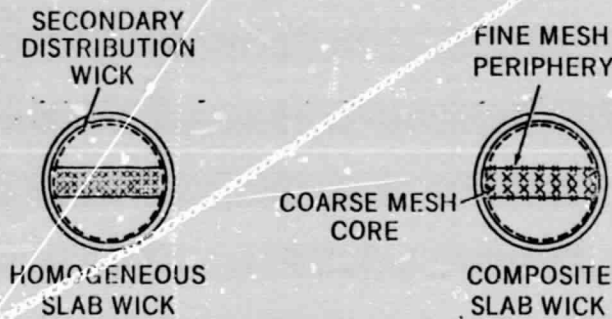


Figure 6. Homogeneous and Composite Slab Wick Designs

In order to provide reliable and easily interpreted 1-g test results, as well as accommodate projected requirements the horizontal slab geometry should satisfy the following criteria:

- 1) Static height ( $H_s$ )  $\geq 1.0\text{-cm} + D_{HP}/2$
- 2) Transport capability  $\sim 3.0\text{ w-m}$  (at 0.2-cm heat pipe elevation (factor of two design margins))
- 3) The composite slab should self-prime at elevations  $\geq 0.2\text{-cm} + D_{HP}/2$

The first criterion is applied to guarantee that the wick will not begin to drain at very shallow elevations and result in puddling effects. This criterion is satisfied if

$$r_p \leq \frac{2\gamma}{H_s} \quad (21)$$

For a 0.635-cm O.D. oxygen pipe a 60 mesh screen size is required. Finer mesh sizes are needed to accommodate larger diameters and/or nitrogen. A calculation of the transport capability based on this first constraint indicates that at best a 1.27-cm O.D. homogeneous slab with oxygen provides marginal transport (i.e. 3.0 w-m) over the temperature range. Nitrogen with its lower transport factor is less than half as good and with a finer mesh screen, is even lower.

The poor performance of the homogeneous wick is due to the low permeability or more appropriately the low ratio of  $k/r_p$  associated with the fine mesh size needed to satisfy the static height requirement. With a composite slab, the outer layer is a fine mesh screen that provides the capillary pumping, whereas the inner core is a more permeable heavier mesh whose pore size is determined by the less stringent self-priming criterion. As a result, composites can provide capacities substantially larger than that afforded by the homogeneous configurations. Figure 7 shows the optimum transport capabilities of 1.27 and 1.0-cm O.D. pipes with oxygen and nitrogen over the applicable temperature range.

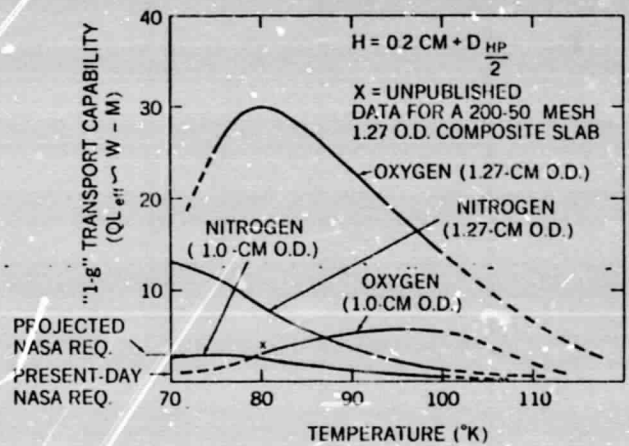


Figure 7. "1-g" Transport Capability vs. Temperature

The optimization is based on using a wick area which maximizes the transport capability. The permeability of the coarse wick is consistent with the mesh size required to satisfy the self-priming criterion (i.e. #3 above), and 200-mesh screen is used for pumping. The 200-mesh was selected because it satisfies the static height requirement for both fluids over the temperature range. It is also approximately the finest mesh size that can be used without having the secondary wick becoming the limiting factor.

The results indicate that oxygen can satisfy the projected transport requirement with either diameter heat pipe. The maximum performance for the 1.27-cm O.D. oxygen pipe is approximately 30 w-m at 80°K, which decreases to 14 w-m at 160°K. Higher vapor losses as well as the reduced wick area result in a maximum ( $QL_{eff}$ ) of 5 w-m for the 1.0-cm pipe with oxygen. The maximum is reached at 95°K when the vapor losses are less dominant.

Nitrogen has a liquid transport factor which is about half that of oxygen's over the temperature range. In addi-

tion its wicking height factor ( $\gamma$ ) is lower and it therefore requires a finer mesh core to satisfy self-priming. This combination results in the lower temperature capability. At 80°K, ( $QL_{eff}$ ) is approximately 8 w-m and this decreases to less than 2 w-m at 100°K with the 1.27-cm O. D. The capacity with the smaller diameter is less than 3 w-m over the entire range. The reduction in capability between the two diameters is less pronounced for nitrogen because it experiences lower vapor losses than oxygen at these temperatures.

A single data point obtained with a comparable 200-50 mesh composite slab with nitrogen in a 1.27-cm O. D. heat pipe is indicated in Figure 7. This pipe had the wick oriented vertically and demonstrated a capability of about 4 w-m in 1-g tests. Although this is only half of the optimized prediction, it does indicate the potential of the basic composite slab. A larger wick area in the test pipe would have resulted in higher performance.

#### Solid Cryogen/Radiant Cooler System

Figure 8 shows schematic diagrams of both a two stage solid cryogen and a hybrid system employing a cryogenic heat pipe. The two stage cooler consists of a primary cryogen (e. g. methane at 90°K) and a secondary cryogen (e. g. ammonia at 160°K) which vent to space. The vent is designed such that the cryogen pressures are always below their triple points. Thus, the cooling process is one of sublimation of the solid cryogen while maintaining the load at a constant temperature. The secondary cryogen maintains an isothermal shroud around the primary cryogen and thus absorbs all external loads to the shroud. The primary cryogen then absorbs all radiative loads from the shroud, the detector assembly, and the conductive load from the secondary cryogen container to which it is mounted. The secondary cryogen must have a higher heat of sublimation than the primary in order for it to offer a weight advantage over a single stage system. Nevertheless, the weight of the secondary cryogen and assembly can be substantial for long duration flights.

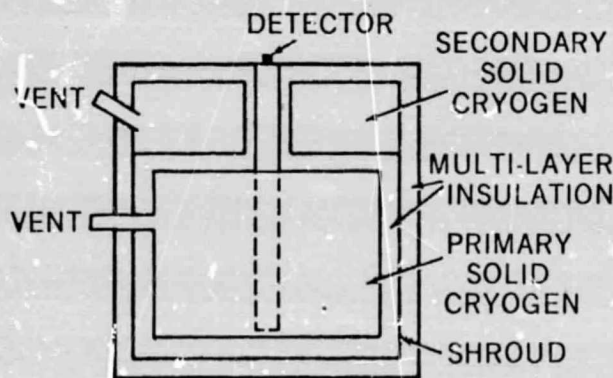


Figure 8a. Two Stage Solid Cryogenic Cooler

A solid cryogen/heat pipe/radiant cooler system as depicted in Figure 8b might be an alternative to the two stage cooler. A device of this nature could be used aboard a spacecraft where the environment precludes the use of a low temperature radiant cooler (~100°K), but would be compatible with a moderate temperature radi-

ator (~160°K). In this system, the low temperature heat pipe and radiator replace the secondary cryogen. The shroud maintains its temperature by transferring its heat load through the heat pipe to the radiator. The heat pipe could be wrapped around the shroud as shown in Figure 8b, or it could interface at a single location. This would depend upon the particular system design and the heat fluxes. In this application, a low temperature heat pipe with possibly ethane as the working fluid (7) would be used. This type of system offers potentially longer life and/or higher load capacities without a prohibitive weight. The following analysis was performed to indicate potential weight savings of the hybrid system compared to a two stage solid cryogen cooler.

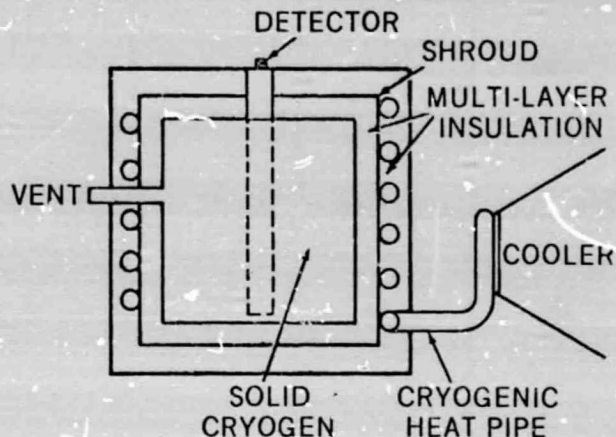


Figure 8b. Heat Pipe/Solid Cryogen System

First, an equation for estimating the weight of the secondary solid cryogen on a two stage system will be developed. For a cylindrically shaped primary solid cryogen of radius,  $r$ , and length,  $l$ ,

$$\frac{A_c}{M} \cong \frac{2\pi(r\ell + r^2)}{\rho_s \pi r^2 \ell} = \frac{1}{\rho_s} \left( \frac{2}{r} + \frac{2}{\ell} \right) \quad (22)$$

Now, assuming  $2r = \ell$ , and neglecting all but radiative heat transfer losses, a heat balance on the primary cryogen yields:

$$\bar{\epsilon} \left( \frac{3}{\rho_s} \right) \sigma (T_1^4 - T_s^4) = \frac{h_s}{T_M} \quad (23)$$

or

$$r = \frac{3T_M \bar{\epsilon}}{\rho_s h_s} \sigma (T_1^4 - T_s^4) \quad (24)$$

Hence,

$$A_c \cong 6\pi r^2 = 54\pi \left\{ \left( \frac{T_M \bar{\epsilon}}{\rho_s h_s} \right) \sigma (T_1^4 - T_s^4) \right\}^2 \quad (25)$$

Again only considering radiant heat transfer for the secondary cryogen

$$\sigma \bar{\epsilon} A_s (T_1^4 - T_s^4) \cong \frac{h_s M^*}{T_M} \quad (26)$$

Combining (25) and (26) and rearranging

$$\frac{M \cdot}{\left(\frac{T_M}{h_s}\right) 54 \pi (\sigma \epsilon)^2 \left(\frac{T_M}{\rho_s h_s}\right)^2 T_E^4 T_s^8} = \left[\left(\frac{T_1}{T_s}\right)^8 \epsilon 2 \left(\frac{T_1}{T_s}\right) + 1\right] \left[1 - \left(\frac{T_1}{T_E}\right)^4\right] \quad (27)$$

For the hybrid system, a heat balance on the solid cryogen and radiator yields

$$\bar{\epsilon} A_c \sigma (T_1^4 - T_s^4) = \frac{M}{T_M} h_s \quad (28)$$

and

$$\bar{\epsilon} A_c \sigma (T_1^4 - T_s^4) + K_3 (T_1 - T_s) \approx \sigma \epsilon_p A_p T_1^4 \quad (29)$$

where we are again only considering radiant heat transfer to the primary cryogen, and conduction and heat pipe inputs to the radiant cooler. In addition, the temperature drop along the heat pipe is neglected, i. e.  $T_p = T_1$ .

Combining (25) and (29)

$$\frac{A_p}{54 \pi \left(\frac{T_M \epsilon \sigma}{\rho_s h_s}\right)^2 \left(\frac{\epsilon}{\epsilon_p}\right) T_1^4 T_s^8} = \left[\left(\frac{T_1}{T_s}\right)^4 - 2 + \left(\frac{T_1}{T_E}\right)^4\right] - \frac{T_1^8}{T_1^4 T_s^4} + 2 \left[\left(\frac{T_1}{T_E}\right)^4 - \left(\frac{T_s}{T_E}\right)^4\right] + \frac{K_3 (T_1 - T_s)}{\sigma \epsilon_p T_1^4} \quad (30)$$

Equations (27) and (30) were used to estimate the weight of the secondary cryogen of a two stage cryogen system, and to compare it to the radiator and heat pipe weight of the hybrid system. Table 1 shows the results of these computations. Although the analysis presented here is but a first cut at evaluating the hybrid cooler system, it appears from this table that for special applications the system offers advantages over a two stage solid cryogenic cooler.

Table 1

Comparison of Secondary Solid Cryogen and Radiant Cooler/Heat Pipe Weights for  $T_1 = 160^\circ\text{K}$

Mission Life	Secondary Cryogen Wt. ( $\epsilon = .007$ )	Radiant Cooler/Heat Pipe Wt.
1 year	11 lbs.	~ 10 lbs.
2 years	87 lbs.	~ 20 lbs.

Heat pipes offer a number of practical advantages in cryogenic radiant cooler systems. However, the parasitic heat loads to the heat pipes require cooler sizes larger than presently used by NASA in the 80 - 100°K temperature range. An optimum heat pipe/radiant cooler will utilize heat pipes that are as small as practical consistent with satisfying transport requirements. The "1-g" test requirements will generally dictate the heat pipe's design. Projected transport requirements for heat pipes in cryogenic NASA coolers are approximately 3 w-m. This requirement along with the need to obtain meaningful "1-g" test results leads to composite wick designs. Axial grooves might also be used but they would have to be designed to provide 2-3 times more pumping in order to avoid "1-g" puddling and obtain good test results in the 80 - 100°K range.

Nitrogen and oxygen are the best fluids for operation over these temperatures. An analysis was performed to determine their performance with an optimized composite slab geometry. The composite slab was selected over an arterial design because it can provide more reliable priming. Results of the analysis indicate that a 1.27-cm O. D. pipe will be required to meet the 3 w-m transport with nitrogen. Although approximately 8 w-m can be obtained with this pipe at 80°K, its performance becomes marginal at 95°K. Oxygen on the other hand can provide an optimized performance of 30 w-m at 80°K which decreases to 19 w-m at 100°K with a 1.27-cm pipe. Even with oxygen, however, the 3 w-m requirement can be satisfied over the temperature range with pipe diameters of 1.0-cm or larger.

An analysis of a solid cryogen/heat pipe/radiant cooler system shows that, for special applications, a weight savings can be realized when compared to a two stage cryogenic system. More design analysis is warranted by this concept.

References

1. Wright, J., and Pence, W., "Development of a Cryogenic Heat Pipe Radiator for a Detector Cooling System," presented at the Intersociety Conference on Environmental Systems, San Diego, California, July 16-19, 1973; ASME paper 47.
2. Brennan, P., Trimmer, D., Sherman, A., and Cygnarowicz, T., "Arterial and Grooved Cryogenic Heat Pipes," ASME paper 71-WA/HT-42, 1971.
3. Murray, D. O., and Foster, W. G., "A Cryogenic Heat Pipe for Satellite Sensor Cooling," presented at the Intersociety Conference on Environmental Systems, San Diego, California, July 16-19, 1973; ASME paper 50.
4. Kroliczek, E. S., and Brennan, P. S., "Axial Grooved Heat Pipes - Cryogenic Through Ambient," ASME paper 73-ENA-48, July 1973.

5. Schlitt, K. R. , Brennan, P. S. , and Kirkpatrick, J. P. , "Parametric Performance of Extruded Axial Grooved Heat Pipes from 80° to 300°K. AIAA/ASME Thermophysics and Heat Transfer Conference, Paper 74-724, July 1974.
6. Heat Pipe Design Handbook, Dynatherm Corp. , DRD No. SE-354T.
7. Kirkpatrick, J. P. and Brennan, P. S. , "The Advanced Thermal Control Flight Experiment," AIAA Paper 73-757, July 1973.